

# TaxDiff: Taxonomic-Guided Diffusion Model for Protein Sequence Generation

Zongying Lin<sup>1</sup> Hao Li<sup>1,2</sup> Liuzhenghao Lv<sup>1</sup> Bin Lin<sup>1</sup> Junwu Zhang<sup>1</sup> Calvin Yu-Chian Chen<sup>1</sup> Li Yuan<sup>1,2</sup>  
Yonghong Tian<sup>1,2</sup>

## Abstract

Designing protein sequences with specific biological functions and structural stability is crucial in biology and chemistry. Generative models already demonstrated their capabilities for reliable protein design. However, previous models are limited to the unconditional generation of protein sequences and lack the controllable generation ability that is vital to biological tasks. In this work, we propose TaxDiff, a taxonomic-guided diffusion model for controllable protein sequence generation that combines biological species information with the generative capabilities of diffusion models to generate structurally stable proteins within the sequence space. Specifically, taxonomic control information is inserted into each layer of the transformer block to achieve fine-grained control. The combination of global and local attention ensures the sequence consistency and structural foldability of taxonomic-specific proteins. Extensive experiments demonstrate that TaxDiff can consistently achieve better performance on multiple protein sequence generation benchmarks in both taxonomic-guided controllable generation and unconditional generation. Remarkably, the sequences generated by TaxDiff even surpass those produced by direct-structure-generation models in terms of confidence based on predicted structures and require only a quarter of the time of models based on the diffusion model. The code for generating proteins and training new versions of TaxDiff is available at: <https://github.com/Linzy19/TaxDiff>.

## 1. Introduction

Protein design (Jumper et al., 2021; Song & Li, 2023; Zheng et al., 2023) aims to generate protein variants with targeted biological functions, which is significant in multiple biological areas, including enzyme reaction catalysis (Repecka

<sup>1</sup>Peking University <sup>2</sup>Peng Cheng Laboratory. Correspondence to: Li Yuan <yuanli-ec@pku.edu.cn>, Yonghong Tian <yhtian@pku.edu.cn>.

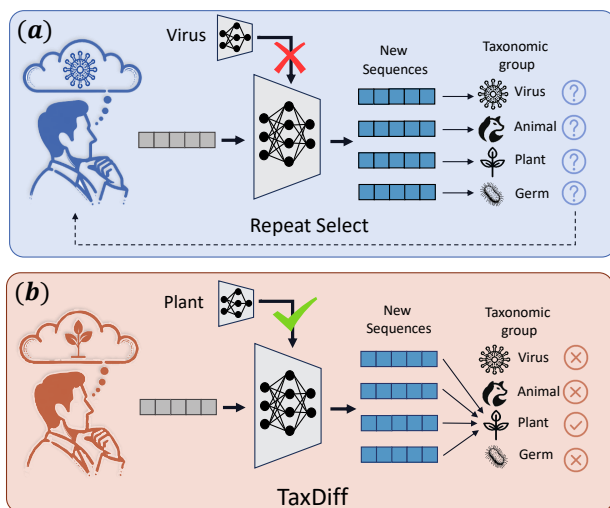


Figure 1. (a). Traditional protein sequence generation models operate without control signals, thus researchers can only randomly generate sequences and subsequently filter them until they fulfill the desired criteria. (b). Our TaxDiff takes species features as guidance for controllable protein sequence generation, meeting the need of biology downstream tasks.

et al., 2021; Fox et al., 2007), vaccine design (Romero & Arnold, 2009; Lin et al., 2022; Phillips et al., 2022), and fluorescence intensity (Biswas et al., 2021; Tan et al., 2023).

Protein design contains two paradigms: sequence generation (Alamdari et al., 2023; Hawkins-Hooker et al., 2021; Repecka et al., 2021) and structure generation (Wu et al., 2022a; Watson et al., 2023). Recently, EvoDiff (Alamdari et al., 2023) proposed a universal designing paradigm, combining structure and sequence generation using the diffusion framework (Song et al., 2020), which improves the protein design efficiency.

Despite the success of EvoDiff (Alamdari et al., 2023) and other sequences generative models (Repecka et al., 2021; Shin et al., 2021; Hawkins-Hooker et al., 2021) that are widely used for designing biologically plausible protein sequences, these protein design models are limited to unconditional generation. As shown in Figure 1.(a), in practical scenes, biological researchers need to filter the randomly generated proteins to fulfill the desired criteria (Huang et al., 2016), which is time-consuming and labor-intensive. Thus,

unconditional protein generation, which can not control protein properties, is still some way from practical application.

To address the uncontrollable challenge, we propose a taxonomic-guided diffusion model, TaxDiff, to design target proteins with the biological-species control signals. Specifically, TaxDiff inserts the taxonomic control features into each Denoise Transformer block of the diffusion model to achieve controllable generation. For fine-grained protein sequence generation, we also propose the patchify attention mechanism in the Denoise Transformer block to capture the protein feature on global and local scales. Furthermore, we reclassify protein sequences at the family and species levels to consolidate the overly detailed classification units within UniProt (uni, 2023). Our TaxDiff follows the protein design paradigm of EvoDiff (Alamdari et al., 2023). Thus, TaxDiff is capable of generating both protein sequences and structures in a shared space.

We carry out extensive experiments to evaluate TaxDiff across multiple benchmarks, encompassing both unconditional and taxonomic-guided controllable protein sequence generation. In unconditional protein sequence generation, the sequence-based TaxDiff demonstrated comparable structural modeling capabilities to structure-based protein generation models, even significantly outperforming them in common metrics such as TM-score, RMSD, and Fident, with improvements of 11.93%, 5.4552, and 7.13% respectively. In taxonomic-guided controllable protein sequence generation, the pLDDT scores from protein structure prediction model OmegaFold (Wu et al., 2022b) far surpassed other sequence generation models, nearing the levels of natural protein sequences. Empirical studies also indicated that due to the patchify attention mechanism, the efficiency of TaxDiff was markedly enhanced, requiring as little as 24 minutes to generate 1000 protein sequences, which is only 1/4 to 2/3 of the time required by other models. All experimental results demonstrate that TaxDiff possesses superior capabilities in exploring protein sequence space and producing structurally coherent proteins. The main contributions of our study are outlined as follows:

- To the best of our knowledge, our TaxDiff is the first controllable protein generation model utilizing guidance from taxonomies.
- Our TaxDiff proposes a taxonomic-guided framework that fits all diffusion-based protein design models. We also propose the patchify attention mechanism for better protein design.
- Experiments demonstrate that our TaxDiff achieves state-of-the-art results in both taxonomic-guided controllable and unconditional protein sequence generation, excelling in structural modeling scores and sequence consistency.

## 2. Related Work

**Diffusion Models** Recently, diffusion models (Ho et al., 2020; Song et al., 2020; Jin et al., 2023) have demonstrated impressive applications and results across various domains, including computer vision (Rombach et al., 2022), natural language generation (Austin et al., 2021), molecular modeling (Luo et al., 2022), and protein structure generation (Watson et al., 2023). The inherent suitability of diffusion models for processing protein structures, coupled with the discrete representation of protein sequences, has led to a predominant focus on structural generation in most current protein studies based on diffusion models, with relatively less attention paid to sequence generation.

**Protein Structures Generation** In recent developments, SMCDiff (Trippe et al., 2022), FrameDiff (Yim et al., 2023), and Liu (2022) employ the graph neural network to generate functional proteins or molecules. Meanwhile, RFDiffusion (Watson et al., 2023) acquires a generative model by fine-tuning the RoseTTAFold structure prediction network (Baek et al., 2021), achieving notable performance across various fields. FoldingDiff (Wu et al., 2022a) describes protein structures through consecutive angles, generating novel structures by denoising from a random, unfolded state. However, a significant limitation in the structure generation paradigm (Ingraham et al., 2023; Lin & AlQuraishi, 2023; Eguchi et al., 2022; Anand & Huang, 2018; Lin et al., 2021), equivalent to the sequence data, there is limited data on protein structures, which restricts the potential exploration of the functional space of proteins. Meanwhile, sequence-based TaxDiff bypasses the bottleneck of limited training data.

**Protein Sequences Generation** Hawkins-Hooker (2021) and Repecka (2021) respectively used VAE and GAN to synthesize functionally active enzyme sequences. Addressing the challenge of nanobodies’ complementarity determining region, Shin (Shin et al., 2021) employed autoregressive models to solve this problem. Wu (2020) and Cao (2021) adopted the Transformer model to design protein sequences. Nevertheless, existing sequence-based models predominantly exhibit limitations to unconditional or specific species (Song & Li, 2023; Hawkins-Hooker et al., 2021) generation. Such constraints underscore a notable gap in the capacity for conditional generation in these models. Through taxonomic guidance, TaxDiff can generate proteins with the biological-species control signals.

## 3. Preliminary

In this section, we first introduce the problem setting of controllable protein sequence generation in Section 3.1, then describe the Diffusion Models (Section 3.2), which is utilized as our main generation framework.

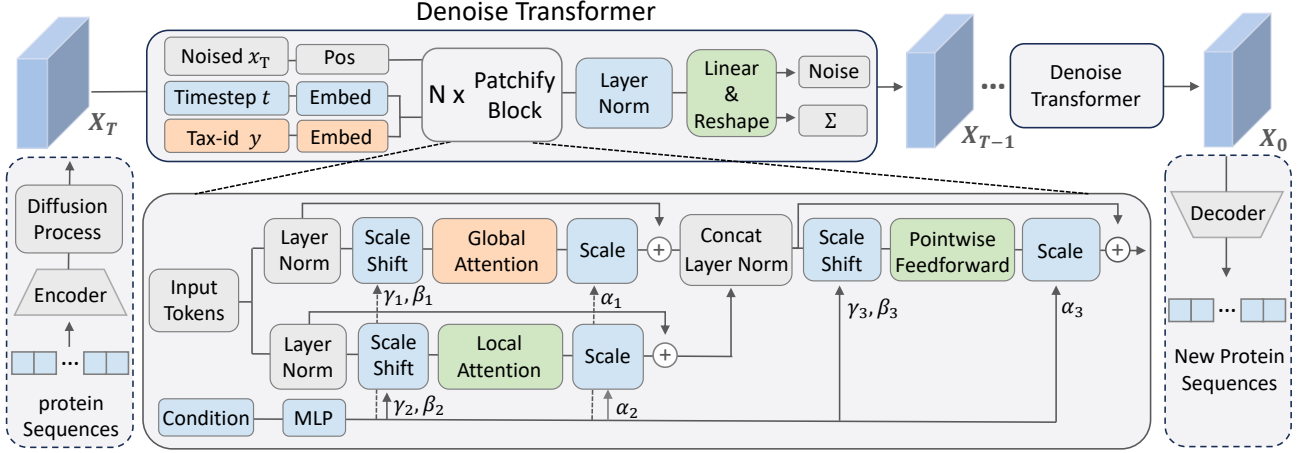


Figure 2. **Overall architecture of the proposed TaxDiff.** This framework delineates how we fuse the Denoise Transformer into the denoising process of the Diffusion model. For a taxonomic-guided controllable generation, we additionally accept a Tax-id  $y$  and embed it with Timestep  $t$  into the Patchify Blocks. The bottom middle of this framework elaborates on the details in Patchify Block.  $\Sigma$  is the predicted diagonal covariance.

### 3.1. Protein Sequence Generation

In this paper, we consider generating protein sequences under the guidance of taxonomies. Protein sequence space can be represented as  $\mathbf{S} = \langle \mathbf{x}, \mathbf{y} \rangle$  where  $\mathbf{x} = (\mathbf{x}_1, \dots, \mathbf{x}_N) \in \mathbf{R}^{N \times L}$  are the protein sequences of length  $L$  and  $\mathbf{y} = (\mathbf{y}_1, \dots, \mathbf{y}_M) \in \mathbf{R}^{M \times 1}$  represents the biological taxonomic category to which the protein belongs, such as Bacteria, Eukaryota, Archaea and so on.  $N$  and  $M$ , respectively represent the total number of protein sequences and categories. We consider the following two generative tasks:

**(I) Unconditional generation.** Using the set of proteins  $\mathbf{x}$ , unconditional generation train parameterized generative models  $p_\theta(\mathbf{x})$  which can randomly generate diverse and realistic protein sequences without other additional labels.

**(II) Controllable generation.** With a collection of protein sequences  $\mathbf{x}$  with label  $\mathbf{y}$ , we build a conditional generative model  $p_\theta(\mathbf{x}|\mathbf{y})$  that is capable of controllable protein sequences generation given desired biological taxonomic category  $\mathbf{y}$ .

### 3.2. Diffusion Model

We briefly introduce the Diffusion Models (DMs) (Sohl-Dickstein et al., 2015; Ho et al., 2020), which is the generation framework of our TaxDiff. DMs are latent variable models (Podell et al., 2023) that model the data  $x_0$  as Markov chains  $x_0 \dots x_T$ , which can be described with two Markovian processes: a forward diffusion process  $q(x_{1:T}|x_0) = \prod_{t=1}^T q(x_t|x_{t-1})$  and a reverse denoising process  $p_\theta(x_{0:T}) = p(x_T) \prod_{t=1}^T p_\theta(x_{t-1}|x_t)$ . The forward process gradually adds Gaussian noise to data  $x_t$ :

$$q(x_t|x_{t-1}) = \mathcal{N}(x_t; \sqrt{\bar{\alpha}_t}x_0, (1 - \bar{\alpha}_t)\mathbf{I}) \quad (1)$$

where the hyperparameter  $\bar{\alpha}_t$  controls the amount of noise added at each timestep  $t$ . The  $\bar{\alpha}_t$  are chosen such that samples  $x_t$  can approximately converge to standard Gaussians  $\mathcal{N}(0, \mathbf{I})$ . Typically, this forward process  $q$  is predefined without trainable parameters.

The generation process of DMs is defined as learning a parameterized reverse denoising process  $p_\theta$ , which aims to incrementally denoise the noisy variables  $x_{T:1}$  to approximate original data  $x_0$  in the target data distribution:

$$p_\theta(x_{t-1}|x_t) = \mathcal{N}(x_{t-1}; \mu_\theta(x_t, t), \Sigma_\theta(x_t, t)) \quad (2)$$

where the initial distribution  $p(x_t)$  is defined as  $\mathcal{N}(0, \mathbf{I})$ . The means  $\mu_\theta$  and variances  $\Sigma_\theta$  typically are neural networks such as U-Nets (Si et al., 2023) for images or Transformers for text (Peebles & Xie, 2023).

## 4. Methodology

We first introduce the framework and data flow of TaxDiff in Section 4.1 and then elucidate the controllable generation under taxonomic-guided in Section 4.2, followed by optimizing the denoise capability of the diffusion model with patchify attention mechanism in Section 4.3. Finally, we will discuss the training procedure, specifically the design of the loss function in Section 4.4. The overall architecture of the proposed TaxDiff is illustrated in Figure 2.

### 4.1. TaxDiff framework

Recognizing the diversity of amino acids, we have introduced an additional dimension  $D$  to enrich features at the amino acid level. Through Encoder, feature-augmented  $x$  can thus be represented as  $x \in \mathbf{R}^{L \times D}$ . In the Denoise

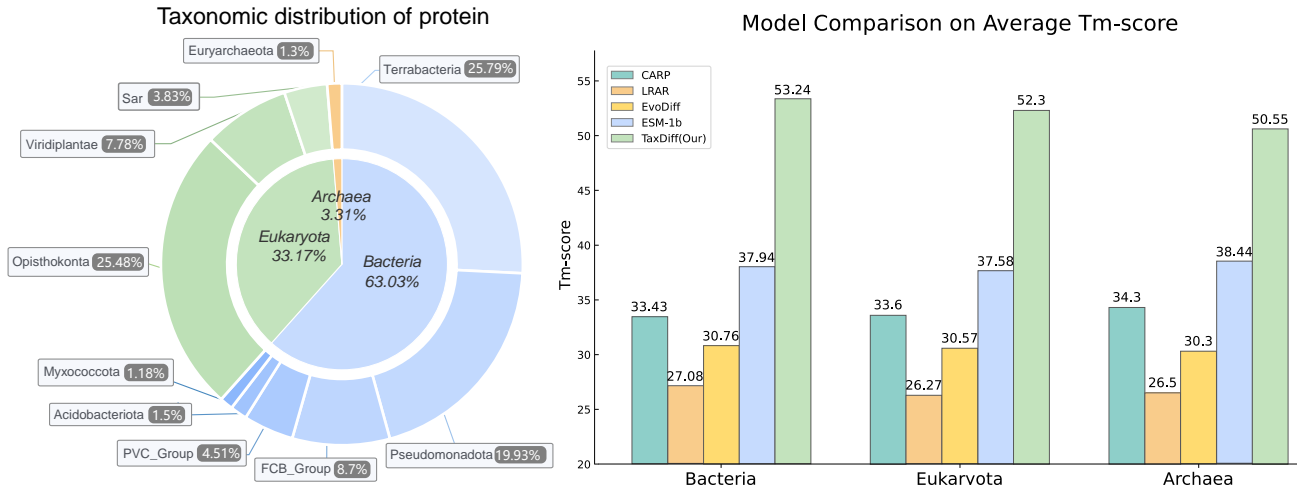


Figure 3. **Taxonomic distribution and comparison of taxonomic-guided models.** *Left:* We display the distribution of species classification from the second and third taxonomic levels, showcasing the top 10 categories. *Right:* We compare the performance of different models in terms of TM-score under the condition of the second taxonomic level.

Transformer block, three different types of inputs are processed: the data  $x_T$  formed by the forward process in DMs that gradually adds Gaussian noise, the timestep  $t$ , and the protein taxonomic identifier  $y$  (tax-id).  $x_T$  undergoes standard Transformer-based frequency position embedding (sine-cosine version) (Dosovitskiy et al., 2020), while the timestep  $t$  and tax-id  $y$  are individually embedded, resulting in two distinct conditional tokens that are concatenated with the  $x_T$ . Conditional tokens are designed for seamless integration, rendering them indistinguishable from protein sequence tokens. After the terminal Patchify block, these conditional tokens are excised from the sequence. This strategy permits the usage of standard Transformer blocks without modification.

After the patchify block, the sequence tokens must be decoded into a predicted noise and diagonal covariance ( $\Sigma$ ). Both of them retain the shape equivalent to that of the original input. To achieve this, adaptive layer normalization (adaLN) (Perez et al., 2018) is applied, and each token is linearly decoded into a tensor of dimensions  $L \times 2D$ . In the decoder, the denoised final result  $\mathbf{x}_0 \in \mathbb{R}^{L \times D}$  is subjected to an argmax layer:  $\text{argmax}(\mathbf{x}_0) \in \mathbb{R}^L$ . The output is then parsed and segmented at each padding or stopping sign, thus generating the protein sequences.

## 4.2. Taxonomic-guided generation

Traditional conditional diffusion models take the class labels or text as extra information (Zhang et al., 2023; Yang et al., 2023), but our TaxDiff encodes tax-id  $y$  as a condition for controllable generation. In this case, the reverse process is formalized as  $p_\theta(x_{t-1}|x_t, y)$ , with both means  $\mu_\theta$  and variances  $\Sigma_\theta$  being conditional by  $y$ . In this way, the taxonomic-guided encourages the sampling pro-

cedure towards maximizing the conditional log-likelihood  $\log p(y|x)$  (Ho & Salimans, 2022). Invoking Bayes’ Rule, we have  $\log p(y|x) \propto \log p(x|y) - \log p(x)$  and hence  $\nabla_x \log p(y|x) \propto \nabla_x \log p(x|y) - \nabla_x \log p(x)$ . DMs based on score functions guides model sample  $x$  with a heightened probability  $p(x|y)$  by adjusting noise prediction:

$$\begin{aligned} \hat{\mu}_\theta(x_t, y) &= \mu_\theta(x_t, \emptyset) + s \cdot \nabla_x \log p(x|y) \\ &\propto \mu_\theta(x_t, \emptyset) + s \cdot (\mu_\theta(x_t, y) - \mu_\theta(x_t, \emptyset)) \end{aligned} \quad (3)$$

where the scalar  $s > 1$  determines the scale of guidance. Notably, setting  $s = 1$  reverts the process to the standard sampling.

As for the DMs with  $y = \emptyset$ , it is done by randomly dropping out  $y$  with a certain probability and replacing it with a ‘null’ embedding  $\emptyset$ . This technique of controllable guided yield significantly improved samples over generic sampling techniques (Ho & Salimans, 2022; Nichol et al., 2021). This observed improvement is also replicated in Figure 3 and Experiments 5.3.

The classification for tax-id  $y$  within UniProt is markedly detailed, resulting in the minimal categories that encompass a limited number of a few. These fine-grained categories hinder effective feature extraction across the broader Taxonomic domain. To address this, we reclassify the ninth layer of original taxonomic lineages, which corresponds to the family and species levels (Luby, 2003). Specifically, we align the protein sequences from UniProt with the taxonomic data from NCBI (Wheeler et al., 2007) by recursive tracing from the terminal child nodes up to the root node, we assign a novel tax-id  $y$  to each sequence. This reorganization effectively condenses the categories to a total of 23,427. Within this refined classification, cellular organ-

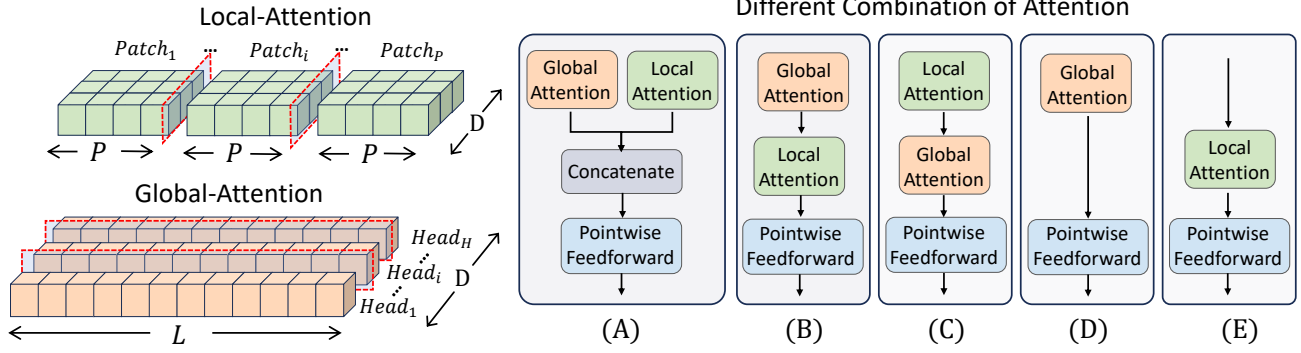


Figure 4. **The patchify attention mechanism.** *Left:* The different division between Local-Attention and Global-Attention. *Right:* we present five different approaches to combining them. The division of the feature dimension in Global-Attention is determined by the number of heads  $H$ , while the number of tokens created by patchifying is determined by the patchify-size  $P$ .

isms represent a predominant 98% of the protein sequences, with the residual 2% attributed to viruses and other entries. Predominant domains within cellular organisms include Bacteria (63%), Eukaryota (33%), and Archaea (3%). Further subdivisions and their respective visual representations are elucidated in Figure. 3 and Appendix A.1.

### 4.3. Patchify attention

To enhance the model’s ability to extract global features of protein sequences and simultaneously preserve the salience of amino-acid local features, we have implemented patchify attention mechanism upon the input protein sequences. This procedure is delineated in Figure 4.

At the protein sequences level, Global-Attention is employed to capture the intricate relationships between different amino acids. For each head  $i$  within the Global-Attention, with a total of  $H$  heads, we calculate the  $Q_i = x \times W_i^Q$ ,  $K_i = x \times W_i^K$  and  $V_i = x \times W_i^V$  as linear transformations of the input matrix  $x \in \mathbb{R}^{L \times D}$ , where  $W_i^Q$ ,  $W_i^K$  and  $W_i^V$  are the weight matrices unique to each head. Attention weights are calculated using the scaled dot-product attention mechanism:

$$Attention_{\text{head}}(Q_i, K_i, V_i) = \text{softmax} \left( \frac{Q_i K_i^T}{\sqrt{d_k}} \right) V_i \quad (4)$$

Here,  $d_k$  is the dimension of the  $K_i$ . The final output of the Global-Attention is procured by concatenating the individual heads’ outputs and subsequently subjecting them to a linear transformation:

$$Global\text{-}Attention(x) = \text{concat}(\text{head}_1, \dots, \text{head}_H) W^O \quad (5)$$

where each head $_i$  represents an attention block, and  $W^O$  serves as an output weight matrix to synthesize all Heads.

At the amino-acids level, Local-Attention divides the sequences of length  $L$  based on the patchify-size  $P$ . For each patch  $j$ , the queries ( $Q_j$ ), keys ( $K_j$ ) and values ( $V_j$ ) are

deduced by:

$$Q_j = \text{Patch}_j(x) \times W_j^Q \quad (6)$$

$$K_j = \text{Patch}_j(x) \times W_j^K \quad (7)$$

$$V_j = \text{Patch}_j(x) \times W_j^V \quad (8)$$

where  $\text{Patch}_j(x)$  signifies the partitioning of  $x$  into its corresponding patch, and  $W_j^Q$ ,  $W_j^K$  and  $W_j^V$  are the patch-specific weight matrices. Attention weights within each patch are also computed utilizing the scaled dot-product attention:

$$Attention_{\text{patch}}(Q_j, K_j, V_j) = \text{softmax} \left( \frac{Q_j K_j^T}{\sqrt{d_k}} \right) V_j \quad (9)$$

where  $d_k$  is the key’s dimension within the patch. The Local-Attention’s ultimate output is derived by concatenating the outputs from all patches:

$$Local\text{-}Attention(x) = \text{concat}(\text{Patch}_1, \dots, \text{Patch}_P) \quad (10)$$

where  $\text{Patch}_j$  equating to  $Attention_{\text{patch}}(Q_j, K_j, V_j)$ .

Additionally, we derive the scaling parameter  $\alpha$  from any residual connections in the Patchify block, while the scaling parameter  $\gamma$  and bias parameter  $\beta$  are regressed from the conditioning embedding vectors of  $t$  and  $y$ . The adaptive layer normalization (adaLN) uniformly applies the same function across all tokens.

To effectively combine Global and Local-Attention, we explored five methodologies for their incorporation and subjected them to extensive experiments. The combinatorial strategies are illustrated in the left of Figure 4: (A) Global-Attention and Local-Attention are used in parallel, with subsequent extracted features concatenation and fusion via Pointwise Feedforward; (B) and (C) Global-Attention and Local-Attention are deploy in a sequential format, capped with Pointwise Feedforward to predict noise and variance; (D) and (E) isolate the utilization to either Global-Attention

Table 1. **Unconditional generation result comparison on AFDB and PDB datasets.** Metrics are calculated with 500 samples generated from each mode. Our TaxDiff best performs on TM-score, RMSD, and Fident for both datasets, and outperforming structure-based RFdiffusion and FoldingDiff on pLDDT.

Architecture	Method	pLDDT $\uparrow$	AFDB Dataset			PDB Dataset		
			TM-score(%) $\uparrow$	RMSD $\downarrow$	Fident(%) $\uparrow$	TM-score(%) $\uparrow$	RMSD $\downarrow$	Fident(%) $\uparrow$
CNN	CARP	34.40 $\pm$ 14.43	25.15	18.8463	14.23	31.21	12.5794	15.34
	LRAR	49.13 $\pm$ 15.50	26.44	18.0071	15.00	30.60	13.1135	15.54
Encoder	ESM-2	51.16 $\pm$ 15.52	25.06	23.6227	17.16	29.47	19.1269	17.41
	ESM-1b	59.57 $\pm$ 15.36	33.24	20.1126	16.94	36.85	16.5417	17.77
Decoder	ProtGPT2	56.32 $\pm$ 16.05	25.79	19.7728	14.48	31.11	13.2589	14.48
	ProGen2	61.07 $\pm$ 18.45	21.59	28.1693	17.68	28.54	18.1132	17.68
Structure	RFdiffusion	57.27 $\pm$ 20.20	30.03	15.8841	13.52	32.58	12.1724	13.76
	FoldingDiff	68.89 $\pm$ 14.60	36.33	11.3627	19.47	37.60	9.2003	20.05
Diffusion	EvoDiff	44.29 $\pm$ 14.51	24.22	20.0326	15.01	29.58	13.9564	15.64
	<b>TaxDiff (Our)</b>	<b>68.89 <math>\pm</math> 9.35</b>	<b>48.26</b>	<b>5.9075</b>	<b>26.60</b>	<b>46.02</b>	<b>4.5736</b>	<b>24.13</b>

or Local-Attention exclusively. The comparison of these five methods and the impact of varying patchify size on local feature extraction capabilities are all explored in the Experiments 5.4.

#### 4.4. Training procedure

The training of diffusion models is aimed to learn the reverse process, which is expressed as  $p_\theta(x_{t-1}|x_t) = \mathcal{N}(\mu_\theta(x_t), \Sigma_\theta(x_t))$ , while the Denoise Transformer is used to estimate  $p_\theta$ . The model training within the variational lower bound of the log-likelihood of  $x_0$ , with the exclusion of an additional term irrelevant for training, the loss function can be represented to:

$$L(\theta) = -p(x_0|x_1) + \sum_t D_{KL}(q^*(x_{t-1}|x_t, x_0) || p_\theta(x_{t-1}|x_t)) \quad (11)$$

Given that both  $q^*$  and  $p_\theta$  are Gaussian, the Kullback–Leibler divergence ( $D_{KL}$ ) can be evaluated by the means and covariances of these distributions.

For simple model training,  $\mu_\theta$  is reparameterized as a noise prediction network  $\epsilon_\theta$ , then the model can be trained using a simple mean-squared error function (MSE loss) between the predicted noise  $\epsilon_\theta(x_t)$  and the actual sampled Gaussian noise  $\epsilon_t$ :

$$L_{MSE}(\theta) = ||\epsilon_\theta(x_t) - \epsilon_t||^2 \quad (12)$$

However, for training diffusion models with a learned reverse process co-variance  $\Sigma_\theta$ , it becomes imperative to optimize the entire  $D_{KL}$  term. Followed DiT (Peebles & Xie, 2023), we train  $\epsilon_\theta$  with  $L_{MSE}$  and  $\Sigma_\theta$  with the full loss function  $L(\theta)$ . Upon the successful training of  $p_\theta$ , new protein sequences can be generated by initializing  $x_t \sim \mathcal{N}(0, I)$  and subsequently sampling  $x_{t-1} \sim p_\theta(x_{t-1}|x_t)$  via the reparameterization trick.

## 5. Experiments

In this section, we justify the advantages of TaxDiff through comprehensive experiments. We begin by presenting our experimental setup in Section 5.1. Subsequently, we report and analyze the outcomes of unconditional and controllable generation in Section 5.2 and Section 5.3, respectively. Finally, We explore various methods of combining Global and Local-Attention, and examine the impact of different patchify-size in Section 5.4.

### 5.1. Experiment Setup

**Datasets:** For our model training, we utilized the Uniref50 dataset from Uniprot (uni, 2023), a protein database formed through clustering. Within TaxDiff, we filter protein sequences in Uniref50 that were less than 256 amino acids in length. Sequences falling short of 256 amino acids undergo zero-padding to equalize their length, thereby standardizing the representation of proteins as sequences with a uniform length  $L = 256$ .

**Setting:** Following the DiT (Peebles & Xie, 2023), we replace the standard layer norm in the Transformer block with adaLN and initialize batch normalization to zero within each Patchify block (adaLN-zero) (Goyal et al., 2017) and employed AdamW (Loshchilov & Hutter, 2017) for training all models. A constant learning rate of  $1 \times 10^{-4}$  without weight decay is used for training, while the batch size is set to 512 on eight 4090 GPUs. Results in Table 1 and Table 2 have the same setup with patchify-size  $P = 16$ , the layer of patchify block  $N = 12$ . More details about setting in Appendix A.2.

**Evaluation:** We measure model performance through the foldability and consistency of sequences generated by TaxDiff. We use Omegafold (Wu et al., 2022b), which relies

Table 2. **Controllable generation on AFDB and PDB datasets.** Metrics are calculated with 1000 samples generated from each model, with lengths following a random distribution between 10 and 256. The sampling time was recorded on a single 4090 for 1000 samples.

Method	pLDDT	Time(mins)↓	AFDB Dataset			PDB Dataset		
			TM-score(%)↑	RMSD↓	Fident(%)↑	TM-score(%)↑	RMSD↓	Fident(%)↑
CARP	46.84 ± 13.35	96.6	33.62	12.5753	12.5	32.38	10.8296	11.82
LRAR	47.33 ± 14.26	79.31	26.94	17.9833	15.83	30.41	13.9929	16.33
Evodiff	56.28 ± 16.52	99.75	30.22	15.8664	16.17	33.02	12.3685	16.29
ESM-1b	67.91 ± 11.59	37.4	37.13	13.6791	16.76	41.90	9.8445	17.27
<b>Taxdiff(Our)</b>	<b>69.00 ± 9.13</b>	<b>24.53</b>	<b>49.27</b>	<b>5.6518</b>	<b>25.02</b>	<b>48.80</b>	<b>4.8453</b>	<b>24.85</b>

only on a single sequence without homologous or evolutionary information, to give the confidence scores(pLDDT) in structure prediction for each residue. Subsequently, Foldseek (van Kempen et al., 2023) calculates the average TM-score, which reflects the structural similarity, and the average RMSD, which focuses on the protein structure size and local variations. Additionally, Foldseek provides the Fident, which serves as sequence-level homology. We choose natural protein structures from the Protein Data Bank (PDB) (Berman et al., 2002) to verify the natural-like degree of generated sequences and high-confidence protein structures predicted by AlphaFold (AFDB) (Jumper et al., 2021; Varadi et al., 2022) to expand the comparison range and verify the broad validity of our model. Settings for results in Table 1 and Table 2 are same. More Details are provided in the Appendix A.3

**Baselines:** We compare TaxDiff to several competitive baseline models. The left-to-right auto regressive (LRAR) and convolutional autoencoding representations of proteins(CARP) (Yang et al., 2022) are both trained with the same dilated convolutional neural network architectures on the UniRef50. FoldingDiff (Wu et al., 2022a) and RFdiffusion (Watson et al., 2023) are recent progress on diffusion models for protein structure generation. Notably, the RFdiffusion and FoldingDiff directly produce protein structures, so we first unconditionally select structures generated by these two and use ESM-IF to design their corresponding sequences. EvoDiff (Alamdari et al., 2023) is a diffusion model combining evolutionary-scale data based on programmable, sequence-first design. ESM-1b (Rao et al., 2021) and state-of-the-art ESM-2 (Lin et al., 2023) are the protein masked language models, which were trained on different releases of UniRef50. ESM series both generated many “unknown” amino acids, and performance was improved results by manually setting the logits for X to inf. ProtGPT2 (Ferruz et al., 2022) and ProGen2 (Nijkamp et al., 2023) are autoregressive large protein language models based on GPT2 (Radford et al., 2019), which have undergone pre-training in UniRef50 and UniRef90 respectively.

## 5.2. Unconditional Sequences Generation

In the unconditional generation, TaxDiff sets the condition  $y$  to be  $\emptyset$  and generates 500 protein sequences within the length range of 10-256. For sequences lengths shorter than 10, we consider them to be invalid protein sequences and, therefore remove them, which is a practice also applicable to sequences generated by all other models.

As shown in Table 1, TaxDiff outperforms competitive baseline methods across all metrics with a noticeable margin. It’s important to note that the sequences generated by our model have exceeded those of the structure generation model RFdiffusion and FoldingDiff in terms of pLDDT. This underscores our model’s efficacy in extracting structural modeling information from protein sequences and substantiates the effectiveness of our sequence-based modeling paradigm. Moreover, in the structural alignment with AFDB and PDB datasets, TaxDiff significantly improves TM-score and RMSD, substantially outperforming other models, especially RMSD, which is less than half that of other models. Furthermore, the sequence consistency Fident also surpasses other models on both two datasets, showcasing the comprehensiveness and generalization capability of our model. Overall, the superior performance demonstrates TaxDiff’s enhanced ability to simulate protein sequence distributions and generate authentic and highly consistent protein sequences.

## 5.3. Taxonomic-Guided Sequences Generation

Under the taxonomic-guided, our objective is to perform controllable protein sequence generation to meet specific needs for proteins of particular species. This can be useful in realistic settings of protein and drug design where we are interested in discovering proteins with specific taxonomic preferences. For a valid comparison, we fine-tune a subset of representative networks with taxonomic-guided and same-label embedding architecture, enabling them to learn the distribution of taxonomic categories. Then, We set the conditional tax-id  $y$  to a fixed random variable representing the taxonomic group to which the protein belongs and generate 1,000 protein sequences to test the model’s controllable generation ability.

Table 3. Contrast experiment of different patchify-size  $P$  in Local-Attention on AFDB and PDB datasets. Metrics are calculated with 1000 samples generated from each model.

Patchify-size	pLDDT $\uparrow$	Time(mins) $\downarrow$	AFDB Dataset			PDB Dataset		
			TM-score $\uparrow$	RMSD $\downarrow$	Fident(%) $\uparrow$	TM-score $\uparrow$	RMSD $\downarrow$	Fident(%) $\uparrow$
4	67.56 $\pm$ 10.35	<b>20.57</b>	46.70	6.8047	23.01	46.58	6.2253	20.57
8	68.88 $\pm$ 9.55	22.94	45.57	6.5407	23.94	46.04	5.4404	22.94
16	69.01 $\pm$ 9.03	24.85	<b>48.88</b>	<b>5.4992</b>	25.88	<b>49.58</b>	<b>4.6262</b>	24.95
32	65.25 $\pm$ 12.12	20.72	42.82	8.094	21.71	43.27	6.8687	20.72
64	<b>70.83 <math>\pm</math> 8.77</b>	24.78	46.48	5.9851	<b>26.16</b>	45.88	5.3077	<b>25.20</b>

We report the numerical results in Table 2. As shown in the table, TaxDiff significantly outperforms baseline models on all the metrics, including the previous diffusion model named EvoDiff, running on the whole Uniref50. The results demonstrate that by taxonomic-guided, not only TaxDiff, almost all models acquired a higher capacity to incorporate given taxonomic information into the generation process. Furthermore, we compare the time to generate 1000 protein sequences with these models. TaxDiff, fusing transformer into diffusion architectures, not only requires less inference time than models relying solely on either the Transformer architecture like ESM-1b or solely on the Diffusion architecture like Evodiff but also significantly outperforms other models in all metrics.

#### 5.4. Sequences Global and Local Attention

In this section, we investigate the impact of different attention combinations on model performance and further analyze the effect of patchify-size at the amino acid level. Specifically, we examine the influence of five different attention combinations in Figure 4 on the protein sequence generation capability. To standardize comparison, except for the experimental variables, we keep other parameters consistent and fix the random seed. This allows the five attention combinations to generate corresponding protein sequences under 1,000 fixed random taxonomic groups. The evaluation of the generated sequences is the same as controllable sequence generation.

The visual comparison in Figure 5 and experimental results in Appendix 4 indicate that the parallel use of Global-Attention and Local-Attention (Method A) achieves the best performance across all metrics, significantly surpassing other combinations. However, it is noteworthy that the exclusive use of Local-Attention (Method E) secures the second-best result, exceeding the performance of what we initially anticipated as the sub-optimal (method B) and (method C). This suggests that for protein sequences, unlike natural language, focusing on local effects using Local-Attention is more effective than applying attention across the entire sequence. It implies that protein sequences also contain “short sentence” like local semantic structures.

To further analyze the impact of different patchify-size on features representation at the amino acid level, we divide sequences by length into segments from 4 to 64, keeping other parameters constant, and use Method A to combine Global-Attention and Local-Attention. We report the numerical results in Table 3. The results demonstrate that dividing protein sequences into 16 amino acids per local patch provides significant advantages for protein structure modeling metrics, such as TM-score and RMSD. In contrast, using a larger patchify size, like dividing protein sequences into 64 amino acids per local patch, has a more substantial impact on improving sequence-related metrics like Fident.

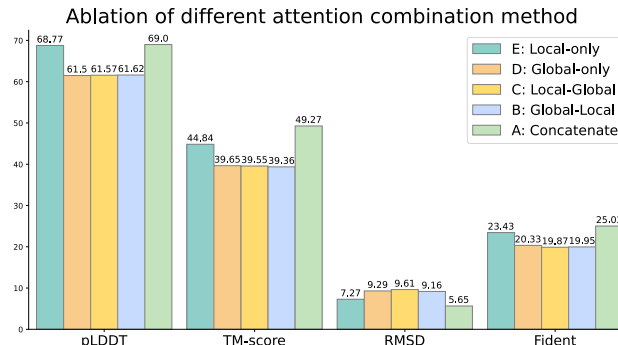


Figure 5. Ablation result of different attention combination on AFDB datasets. Metrics are calculated with 1000 samples generated from each model.

## 6. Conclusion and Future Work

While current models can only perform unconditional sequence generation, TaxDiff overcomes this limitation by learning taxonomic-guided over protein sequences space. By combining the Global-Attention to sequences and Local-Attention to amino acids, TaxDiff can effectively generate sequences that are structurally reliable and consistent in sequence. Furthermore, TaxDiff requires only a quarter of the time needed by other diffusion-based models to achieve superior performance. Various experimental results demonstrate its significantly better ability for modeling natural protein sequences. As a versatile and principled framework, TaxDiff can be expanded for various protein generation applications in future work. For instance, scaling up TaxDiff to the more challenging protein generation of protein complex.



## Impact Statements

Our work with biological protein sequences aims to advance the field of machine learning and introduce machine learning into traditional scientific neighborhoods as a way to promote and robust the AI for science community and accelerate research in the basic sciences.

Our model TaxDiff, a taxonomy-guided protein sequence generation model can greatly reduce screening time for biological researchers and facilitate drug and new protein design.

At the same time, however, our work is based on generative models that learn the feature space of protein sequences and use it to generate new protein sequences that may not be easily expressed and synthesized in the lab.

## References

- Uniprot: the universal protein knowledgebase in 2023. *Nucleic Acids Research*, 51(D1):D523–D531, 2023.
- Alamdari, S., Thakkar, N., van den Berg, R., Lu, A. X., Fusi, N., Amini, A. P., and Yang, K. K. Protein generation with evolutionary diffusion: sequence is all you need. *bioRxiv*, pp. 2023–09, 2023.
- Anand, N. and Huang, P. Generative modeling for protein structures. *Advances in neural information processing systems*, 31, 2018.
- Austin, J., Johnson, D. D., Ho, J., Tarlow, D., and Van Den Berg, R. Structured denoising diffusion models in discrete state-spaces. *Advances in Neural Information Processing Systems*, 34:17981–17993, 2021.
- Baek, M., DiMaio, F., Anishchenko, I., Dauparas, J., Ovchinnikov, S., Lee, G. R., Wang, J., Cong, Q., Kinch, L. N., Schaeffer, R. D., et al. Accurate prediction of protein structures and interactions using a three-track neural network. *Science*, 373(6557):871–876, 2021.
- Berman, H. M., Battistuz, T., Bhat, T. N., Bluhm, W. F., Bourne, P. E., Burkhardt, K., Feng, Z., Gilliland, G. L., Iype, L., Jain, S., et al. The protein data bank. *Acta Crystallographica Section D: Biological Crystallography*, 58(6):899–907, 2002.
- Biswas, S., Khimulya, G., Alley, E. C., Esvelt, K. M., and Church, G. M. Low-n protein engineering with data-efficient deep learning. *Nature methods*, 18(4):389–396, 2021.
- Cao, Y., Das, P., Chenthamarakshan, V., Chen, P.-Y., Melnyk, I., and Shen, Y. Fold2seq: A joint sequence (1d)-fold (3d) embedding-based generative model for protein design. In *International Conference on Machine Learning*, pp. 1261–1271. PMLR, 2021.
- Dosovitskiy, A., Beyer, L., Kolesnikov, A., Weissenborn, D., Zhai, X., Unterthiner, T., Dehghani, M., Minderer, M., Heigold, G., Gelly, S., et al. An image is worth 16x16 words: Transformers for image recognition at scale. *arXiv preprint arXiv:2010.11929*, 2020.
- Eguchi, R. R., Choe, C. A., and Huang, P.-S. Ig-vae: Generative modeling of protein structure by direct 3d coordinate generation. *PLoS computational biology*, 18(6): e1010271, 2022.
- Ferruz, N., Schmidt, S., and Höcker, B. Protgpt2 is a deep unsupervised language model for protein design. *Nature communications*, 13(1):4348, 2022.
- Fox, R. J., Davis, S. C., Mundorff, E. C., Newman, L. M., Gavrilovic, V., Ma, S. K., Chung, L. M., Ching, C., Tam, S., Muley, S., et al. Improving catalytic function by prosar-driven enzyme evolution. *Nature biotechnology*, 25(3):338–344, 2007.
- Goyal, P., Dollár, P., Girshick, R., Noordhuis, P., Wesolowski, L., Kyrola, A., Tulloch, A., Jia, Y., and He, K. Accurate, large minibatch sgd: Training imagenet in 1 hour. *arXiv preprint arXiv:1706.02677*, 2017.
- Hawkins-Hooker, A., Depardieu, F., Baur, S., Couairon, G., Chen, A., and Bikard, D. Generating functional protein variants with variational autoencoders. *PLoS computational biology*, 17(2):e1008736, 2021.
- Ho, J. and Salimans, T. Classifier-free diffusion guidance. *arXiv preprint arXiv:2207.12598*, 2022.
- Ho, J., Jain, A., and Abbeel, P. Denoising diffusion probabilistic models. *Advances in neural information processing systems*, 33:6840–6851, 2020.
- Huang, P.-S., Boyken, S. E., and Baker, D. The coming of age of de novo protein design. *Nature*, 537(7620): 320–327, 2016.
- Ingraham, J. B., Baranov, M., Costello, Z., Barber, K. W., Wang, W., Ismail, A., Frappier, V., Lord, D. M., Ng-Thow-Hing, C., Van Vlack, E. R., et al. Illuminating protein space with a programmable generative model. *Nature*, pp. 1–9, 2023.
- Jin, P., Li, H., Cheng, Z., Li, K., Ji, X., Liu, C., Yuan, L., and Chen, J. Diffusionret: Generative text-video retrieval with diffusion model. *arXiv preprint arXiv:2303.09867*, 2023.
- Jumper, J., Evans, R., Pritzel, A., Green, T., Figurnov, M., Ronneberger, O., Tunyasuvunakool, K., Bates, R., Židek, A., Potapenko, A., et al. Highly accurate protein structure prediction with alphafold. *Nature*, 596(7873):583–589, 2021.

- Lin, Y. and AlQuraishi, M. Generating novel, designable, and diverse protein structures by equivariantly diffusing oriented residue clouds. *arXiv preprint arXiv:2301.12485*, 2023.
- Lin, Z., Sercu, T., LeCun, Y., and Rives, A. Deep generative models create new and diverse protein structures. In *Machine Learning for Structural Biology Workshop, NeurIPS*, 2021.
- Lin, Z., Akin, H., Rao, R., Hie, B., Zhu, Z., Lu, W., dos Santos Costa, A., Fazel-Zarandi, M., Sercu, T., Candido, S., et al. Language models of protein sequences at the scale of evolution enable accurate structure prediction. *BioRxiv*, 2022:500902, 2022.
- Lin, Z., Akin, H., Rao, R., Hie, B., Zhu, Z., Lu, W., Smetanin, N., Verkuil, R., Kabeli, O., Shmueli, Y., et al. Evolutionary-scale prediction of atomic-level protein structure with a language model. *Science*, 379(6637): 1123–1130, 2023.
- Liu, M., Luo, Y., Uchino, K., Maruhashi, K., and Ji, S. Generating 3d molecules for target protein binding. *arXiv preprint arXiv:2204.09410*, 2022.
- Loshchilov, I. and Hutter, F. Decoupled weight decay regularization. *arXiv preprint arXiv:1711.05101*, 2017.
- Luby, J. J. Taxonomic classification and brief history. In *Apples: botany, production and uses*, pp. 1–14. Cabi Publishing Wallingford UK, 2003.
- Luo, S., Su, Y., Peng, X., Wang, S., Peng, J., and Ma, J. Antigen-specific antibody design and optimization with diffusion-based generative models for protein structures. *Advances in Neural Information Processing Systems*, 35: 9754–9767, 2022.
- Nichol, A., Dhariwal, P., Ramesh, A., Shyam, P., Mishkin, P., McGrew, B., Sutskever, I., and Chen, M. Glide: Towards photorealistic image generation and editing with text-guided diffusion models. *arXiv preprint arXiv:2112.10741*, 2021.
- Nijkamp, E., Ruffolo, J. A., Weinstein, E. N., Naik, N., and Madani, A. Progen2: exploring the boundaries of protein language models. *Cell Systems*, 14(11):968–978, 2023.
- Peebles, W. and Xie, S. Scalable diffusion models with transformers. In *Proceedings of the IEEE/CVF International Conference on Computer Vision*, pp. 4195–4205, 2023.
- Perez, E., Strub, F., De Vries, H., Dumoulin, V., and Courville, A. Film: Visual reasoning with a general conditioning layer. In *Proceedings of the AAAI conference on artificial intelligence*, volume 32, 2018.
- Phillips, D., Gasser, H.-C., Kamp, S., Pałkowski, A., Rabalski, L., Oyarzún, D. A., Rajan, A., and Alfaro, J. A. Generating immune-aware sars-cov-2 spike proteins for universal vaccine design. In *Workshop on Healthcare AI and COVID-19*, pp. 100–116. PMLR, 2022.
- Podell, D., English, Z., Lacey, K., Blattmann, A., Dockhorn, T., Müller, J., Penna, J., and Rombach, R. Sdxl: Improving latent diffusion models for high-resolution image synthesis. *arXiv preprint arXiv:2307.01952*, 2023.
- Radford, A., Wu, J., Child, R., Luan, D., Amodei, D., Sutskever, I., et al. Language models are unsupervised multitask learners. *OpenAI blog*, 1(8):9, 2019.
- Rao, R. M., Liu, J., Verkuil, R., Meier, J., Canny, J., Abbeel, P., Sercu, T., and Rives, A. Msa transformer. In *International Conference on Machine Learning*, pp. 8844–8856. PMLR, 2021.
- Repecka, D., Jauniskis, V., Karpus, L., Rembeza, E., Rokaitis, I., Zrimec, J., Poviloniene, S., Laurynenas, A., Viknander, S., Abuajwa, W., et al. Expanding functional protein sequence spaces using generative adversarial networks. *Nature Machine Intelligence*, 3(4):324–333, 2021.
- Rombach, R., Blattmann, A., Lorenz, D., Esser, P., and Ommer, B. High-resolution image synthesis with latent diffusion models. In *Proceedings of the IEEE/CVF conference on computer vision and pattern recognition*, pp. 10684–10695, 2022.
- Romero, P. A. and Arnold, F. H. Exploring protein fitness landscapes by directed evolution. *Nature reviews Molecular cell biology*, 10(12):866–876, 2009.
- Shin, J.-E., Riesselman, A. J., Kollasch, A. W., McMahon, C., Simon, E., Sander, C., Manglik, A., Kruse, A. C., and Marks, D. S. Protein design and variant prediction using autoregressive generative models. *Nature communications*, 12(1):2403, 2021.
- Si, C., Huang, Z., Jiang, Y., and Liu, Z. Freeu: Free lunch in diffusion u-net. *arXiv preprint arXiv:2309.11497*, 2023.
- Sohl-Dickstein, J., Weiss, E., Maheswaranathan, N., and Ganguli, S. Deep unsupervised learning using nonequilibrium thermodynamics. In *International conference on machine learning*, pp. 2256–2265. PMLR, 2015.
- Song, Y., Sohl-Dickstein, J., Kingma, D. P., Kumar, A., Ermon, S., and Poole, B. Score-based generative modeling through stochastic differential equations. *arXiv preprint arXiv:2011.13456*, 2020.
- Song, Z. and Li, L. Importance weighted expectation-maximization for protein sequence design. *arXiv preprint arXiv:2305.00386*, 2023.

- Tan, Z., Li, Y., Wu, X., Zhang, Z., Shi, W., Yang, S., and Zhang, W. De novo creation of fluorescent molecules via adversarial generative modeling. *RSC advances*, 13(2): 1031–1040, 2023.
- Trippe, B. L., Yim, J., Tischer, D., Baker, D., Broderick, T., Barzilay, R., and Jaakkola, T. Diffusion probabilistic modeling of protein backbones in 3d for the motif-scaffolding problem. *arXiv preprint arXiv:2206.04119*, 2022.
- van Kempen, M., Kim, S. S., Tumescheit, C., Mirdita, M., Lee, J., Gilchrist, C. L., Söding, J., and Steinegger, M. Fast and accurate protein structure search with foldseek. *Nature Biotechnology*, pp. 1–4, 2023.
- Varadi, M., Anyango, S., Deshpande, M., Nair, S., Natassia, C., Yordanova, G., Yuan, D., Stroe, O., Wood, G., Laydon, A., et al. AlphaFold protein structure database: massively expanding the structural coverage of protein-sequence space with high-accuracy models. *Nucleic acids research*, 50(D1):D439–D444, 2022.
- Watson, J. L., Juergens, D., Bennett, N. R., Trippe, B. L., Yim, J., Eisenach, H. E., Ahern, W., Borst, A. J., Ragotte, R. J., Milles, L. F., et al. De novo design of protein structure and function with rfdiffusion. *Nature*, 620(7976): 1089–1100, 2023.
- Wheeler, D. L., Barrett, T., Benson, D. A., Bryant, S. H., Canese, K., Chetvermin, V., Church, D. M., DiCuccio, M., Edgar, R., Federhen, S., et al. Database resources of the national center for biotechnology information. *Nucleic acids research*, 35(suppl\_1):D5–D12, 2007.
- Wu, K. E., Yang, K. K., Berg, R. v. d., Zou, J. Y., Lu, A. X., and Amini, A. P. Protein structure generation via folding diffusion. *arXiv preprint arXiv:2209.15611*, 2022a.
- Wu, R., Ding, F., Wang, R., Shen, R., Zhang, X., Luo, S., Su, C., Wu, Z., Xie, Q., Berger, B., Ma, J., and Peng, J. High-resolution de novo structure prediction from primary sequence. *bioRxiv*, 2022b. doi: 10.1101/2022.07.21.500999. URL <https://www.biorxiv.org/content/early/2022/07/22/2022.07.21.500999>.
- Wu, Z., Yang, K. K., Liszka, M. J., Lee, A., Batzilla, A., Wernick, D., Weiner, D. P., and Arnold, F. H. Signal peptides generated by attention-based neural networks. *ACS Synthetic Biology*, 9(8):2154–2161, 2020.
- Yang, K. K., Fusi, N., and Lu, A. X. Convolutions are competitive with transformers for protein sequence pre-training. *bioRxiv*, pp. 2022–05, 2022.
- Yang, L., Zhang, Z., Song, Y., Hong, S., Xu, R., Zhao, Y., Zhang, W., Cui, B., and Yang, M.-H. Diffusion models: A comprehensive survey of methods and applications. *ACM Computing Surveys*, 56(4):1–39, 2023.
- Yim, J., Trippe, B. L., De Bortoli, V., Mathieu, E., Doucet, A., Barzilay, R., and Jaakkola, T. Se (3) diffusion model with application to protein backbone generation. *arXiv preprint arXiv:2302.02277*, 2023.
- Zhang, L., Rao, A., and Agrawala, M. Adding conditional control to text-to-image diffusion models. In *Proceedings of the IEEE/CVF International Conference on Computer Vision*, pp. 3836–3847, 2023.
- Zhang, Y. and Skolnick, J. Scoring function for automated assessment of protein structure template quality. *Proteins: Structure, Function, and Bioinformatics*, 57(4):702–710, 2004.
- Zheng, Z., Deng, Y., Xue, D., Zhou, Y., Ye, F., and Gu, Q. Structure-informed language models are protein designers. *bioRxiv*, pp. 2023–02, 2023.

## A. Appendix.

### A.1. Result and visualization

Taxonomic distribution and comparison of taxonomic-guided models. More details of refined classification results will be available in supplementary material and website <https://github.com/Linzy19/TaxDiff>.

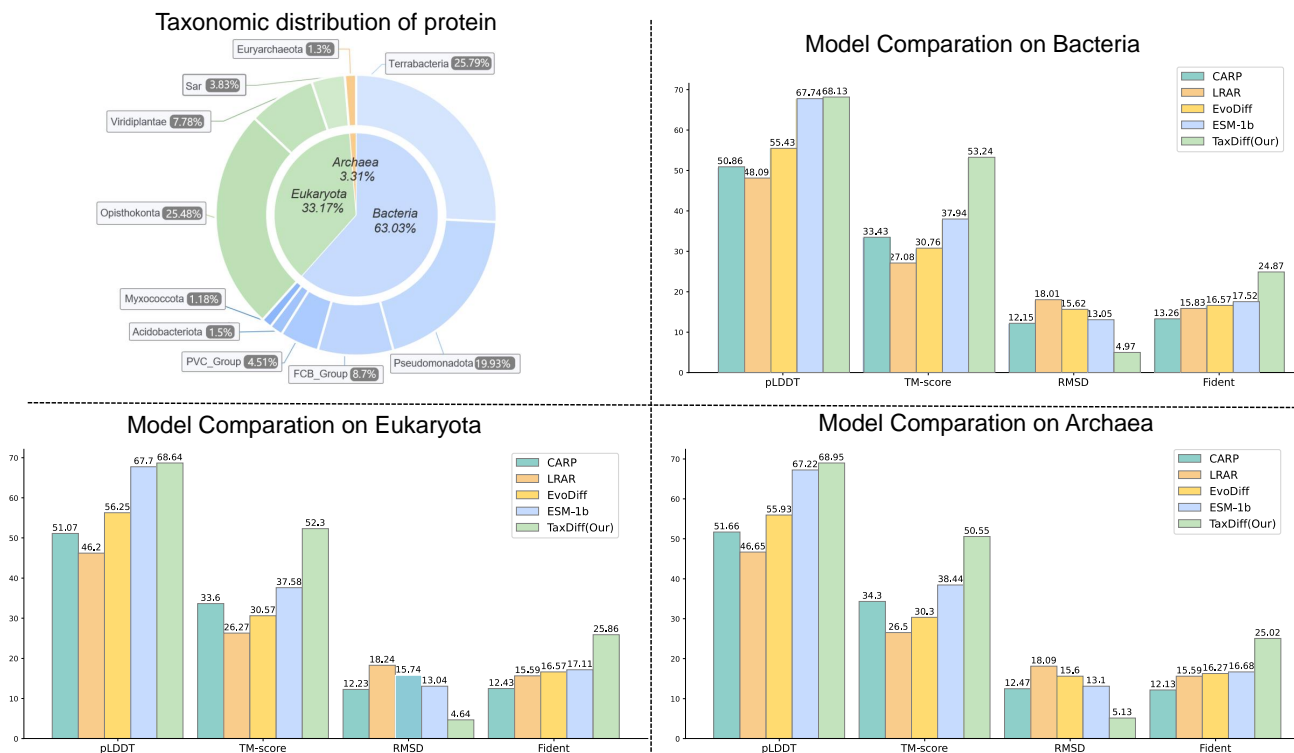


**Figure 6. Taxonomic distribution and comparison of taxonomic-guided models.** *Top Left:* We display the distribution of species classification from the second and third taxonomic levels, showcasing the top 10 categories. In the bar graph, we compare the performance of different models under the condition of the second taxonomic level.

### A.2. Experiment setting

Following common practices in generative modeling literature, we maintained an exponential moving average (EMA) of the TaxDiff weights during training, with a decay factor of 0.9999. The same training hyperparameters were applied across all TaxDiff models and patch sizes. All reported results are based on the EMA model. The same training hyperparameters were applied across all TaxDiff model sizes and patch sizes, almost entirely retained from ADM, without adjustments in learning rate, decay/warm-up schedule, Adam  $\beta_1, \beta_2, \beta_3$ , or weight decay.

### A.3. Evaluation

We measure model performance through sequence consistency and structural foldability, which indicates whether the model can learn the rules of protein sequences from the data. For assessing the feasibility of the sequences, We employed OmegaFold (Wu et al., 2022b) to predict their corresponding structures and calculate the average predicted Local Distance Difference Test (pLDDT) across the entire structure, which reflects OmegaFold’s confidence in its structure prediction for each residue on sequences level. Omegafold performs structure prediction without the need for homologous sequences or evolutionary information, relying solely on a single sequence for prediction. However, due to inherent noise and errors in OmegaFold’s structure predictions, which only consider the foldability of individual sequences, we further measure our results using Foldseek (van Kempen et al., 2023). Foldseek facilitates the pairing of the queried protein  $p^{query}$  with

structurally similar proteins from an existing protein database, yielding pairs represented as  $(p^{query}, p^{target})$ . Here,  $p^{target}$  denotes the protein in the database with a significant structural similarity to  $p^{query}$ . The magnitude of the average template modeling score (TM-score (Zhang & Skolnick, 2004)) value and root-mean-square deviation (RMSD) reflects the degree of structural similarity. TM-score takes into account the overall topological structure of proteins, focusing more on the protein’s overall structure. RMSD calculates the square root of the average position deviation of corresponding atoms between two protein structures, being highly sensitive to the size of the protein structure and local variations. Additionally, Foldseek also calculates the sequence identity (FIDENT) between  $p^{query}$  and  $p^{target}$ , reflecting their sequence-level similarity. In Foldseek, we choose natural protein structures from the Protein Data Bank (PDB) (Berman et al., 2002) to verify the natural-like degree of our sequences and high-confidence protein structures predicted by AlphaFold (AFDB) (Jumper et al., 2021) to expand the comparison range and verify the broad validity of our model.

#### A.4. Ablation result

Table 4. Ablation result of different attention combination on AFDB and PDB datasets. Metrics are calculated with 1000 samples generated from each model.

Method	pLDDT $\uparrow$	AFDB Dataset			PDB Dataset		
		TM-score $\uparrow$	RMSD $\downarrow$	Fident(%) $\uparrow$	TM-score $\uparrow$	RMSD $\downarrow$	Fident(%) $\uparrow$
E	68.77 $\pm$ 10.67	44.84	7.2685	23.43	44.00	5.9162	24.1
D	61.50 $\pm$ 13.55	39.65	9.2808	20.33	39.30	7.6774	19.53
C	61.57 $\pm$ 12.99	39.55	9.6091	19.87	40.21	7.6458	20.12
B	61.62 $\pm$ 12.99	39.36	9.1560	19.95	40.52	7.551	19.77
A	<b>69.01 <math>\pm</math> 9.03</b>	<b>48.88</b>	<b>5.4992</b>	<b>25.88</b>	<b>49.58</b>	<b>4.6262</b>	<b>24.95</b>